Iminoaminosulfinates: Synthesis, Crystal Structures, and Rearrangement monitored by Lithium-7 Solid-state Nuclear Magnetic Resonance Spectroscopy†

Stefanie Freitag,[a] Waclaw Kolodziejski,[b] Frank Pauer[a] and Dietmar Stalke[*,a]

[a] Institut für Anorganische Chemie der Universität Göttingen, Tammannstrasse 4, D-37077 Göttingen, Germany

[b] Department of Chemistry, University of Cambridge, Lensfield Road, Cambridge CB2 1EW, UK

Alkali- and alkaline-earth-metal iminoaminosulfinates have been synthesised and characterized by X-ray diffraction and solid-state NMR investigations. The viability of metal-exchange reactions has been demonstrated resulting in a magnesium and a copper(I) derivative. The structural investigations reveal the presence of different structures, which can be classified into four types. Phase transitions between different structural types involving the loss of donor solvent have been observed by solid-state magic angle spinning experiments.

Alkali-metal iminoaminosulfinates (sulfinamidinates) are widely used in main-group and transition-metal chemistry[1-5] because of their favourable solubility in hydrocarbons and their steric requirements similar to those of the cyclopentadienyl ligand. They assume four different structural types.[6] Most of them are dimers, which differ in the way they associate. According to Fig. 1, these can be classified into a twisted tricyclic structure **a** with C_2 symmetry, a ladder or step structure **b**, and an eight-membered ring structure **c**. The last two types exhibit C_i symmetry. Also, the structure of the lithium lithiate $[Li(12\text{-crown-4})_2]^+[Li\{(NSiMe_3)_2SPh\}_2]^-$ (12-crown-4 = 1,4,7,10-tetraoxacyclododecane) has been reported and classified as of type **d**.[7] It consists of a crown ether-complexed lithium cation and an anionic moiety in which lithium is bonded to two chelating iminoaminosulfinate anions, affording an overall singly charged anion of the 'ate' type.[8]

Our aim was to obtain compounds with 'tailor-made' reactivity. Thus a series of compounds containing the alkali metals Li, Na, K, Rb and Cs was synthesized and structurally characterized[6,9] (see Table 1). In order to extend this system to alkaline-earth metals and to investigate the viability of metal-exchange reactions the compounds $\{MgBr[(Me_3SiN)_2SPh]\cdot thf\}_2$ **8** and $Mg[(Me_3SiN)_2SPh]_2\cdot thf$ **9** have now been prepared and structurally characterized. Recently, we investigated the properties of iminoaminosulfinates in alkali-metal derivatives both in the solid state and in solution. In addition, the protonated species $PhS(NHBu^t)(NSiMe_3)$ **1b**[6] was prepared and structurally characterized. The structure of $PhS(NHSiMe_3)(NSiMe_3)$ **1a** is now reported.

The use of Bu^t as the substituent on S has a marked steric influence on the structure. Depending on the R″ group, there is a transition from an eight-membered ring (type **c**) to a stair-shaped tricycle (type **b**) in the series **2b**, **2a**, **2c** (described here) where R″ = Bu^t, $SiMe_3$ and C_6H_{11}, respectively, of decreasing steric demands. In all these cases, no Et_2O molecule bonds to lithium, although the syntheses were carried out in this solvent. Four instances of type **a** are present in Table 1. The crystal structures of two, **3c** and **4b**, and NMR investigations on **3a** and **3c** are reported in this paper. The influence of R″ on the
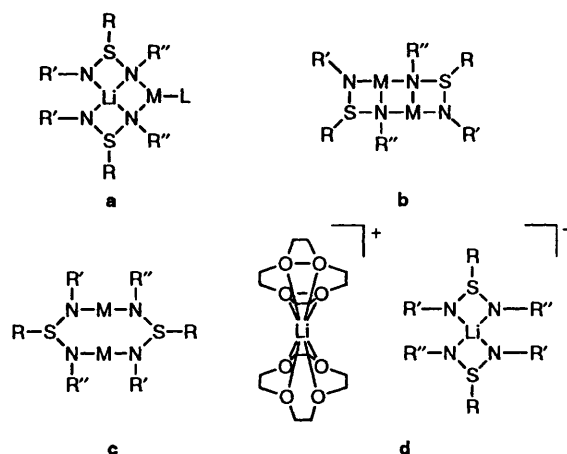
structure of series **3a**–**3c** is less dramatic than in **2a**–**2c** (see Tables 3 and 4).

Solid-state NMR experiments provide the opportunity to observe dynamic processes. For the lithium lithiate **3e** (type **d**) three different signals in the solid-state NMR spectrum were detected and assigned for the first time.[7] Here we present the results of solid-state NMR investigations on the lithiumimino-aminosulfinates **3a** and **3c**.
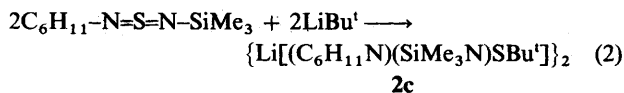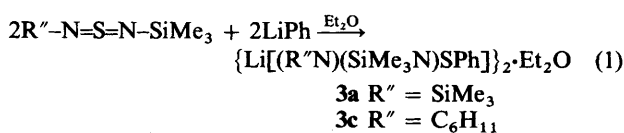
For the lithium to the caesium derivatives, the following trends have been previously identified:[6] the stair angle between the central M_2N_2 and the peripheral SN_2M ring planes becomes more acute; the phenyl ring turns towards the metal atom of the other monomeric unit, as can be seen from the torsion angle N(1)–S(1)–C(1)–C(6) [Fig. 2(b)]; in the series **3d** (M = Li), **4a** (Na), **5a** (K), **6** (Rb), **7** (Cs). For the M–N distances the M(1)–N(2a) distance increases more than the average, which enables the metal to move from the ipso-carbon atom to the ring centre [Fig. 2(a)].

Results and Discussion

The dimers **3a**,[6] **3c**, and **2c** have been prepared by the reactions (1) and (2). All products are obtained in both high yield and

Fig. 1 Structural types of iminoaminosulfinates; M = metal, L = donor ligand

$$2R''-N=S=N-SiMe_3 + 2LiPh \xrightarrow{Et_2O}$$
$$\{Li[(R''N)(SiMe_3N)SPh]\}_2 \cdot Et_2O \quad (1)$$
$$\mathbf{3a} \ R'' = SiMe_3$$
$$\mathbf{3c} \ R'' = C_6H_{11}$$

$$2C_6H_{11}-N=S=N-SiMe_3 + 2LiBu^t \longrightarrow$$
$$\{Li[(C_6H_{11}N)(SiMe_3N)SBu^t]\}_2 \quad (2)$$
$$\mathbf{2c}$$

purity. The reaction of **1a** and half an equivalent of **3a** with NaH in 1,2-dimethoxyethane (dme) leads to the formation of the mixed-metal iminoaminosulfinate **4b** [equation (3)]. Deproton-
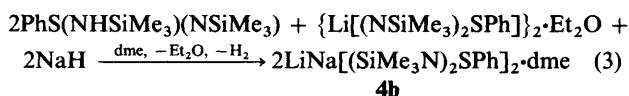
$$2PhS(NHSiMe_3)(NSiMe_3) + \{Li[(NSiMe_3)_2SPh]\}_2 \cdot Et_2O +$$
$$2NaH \xrightarrow{dme, \ -Et_2O, \ -H_2} 2LiNa[(SiMe_3N)_2SPh]_2 \cdot dme \quad (3)$$
$$\mathbf{4b}$$

Table 1 Alkali-metal iminoaminosulfinates; R' = SiMe₃ in all compounds

R
|
S
R'—N⟨ ⟩N—R''
M
|
L

Compound	M	R	R''	Donor L	Structural type	Ref.
2a	Li	Bu^t	SiMe₃	—	b	6
2b	Li	Bu^t	Bu^t	—	c	6
2c	Li	Bu^t	C₆H₁₁	—	b	This work
3a	Li	Ph	SiMe₃	Et₂O	a	9
3b	Li	Ph	Bu^t	Et₂O	a	9
3c	Li	Ph	C₆H₁₁	Et₂O	a	This work
3d	Li	Ph	SiMe₃	thf	b	9
3e	Li	Ph	SiMe₃	12-crown-4	d	7
4a	Na	Ph	Bu^t	thf	b	6
4b	Li/Na	Ph	SiMe₃	dme	a	This work
5a	K	Ph	Bu^t	thf	b	6
5b	K	Ph	SiMe₃	dme	b	This work
6	Rb	Ph	SiMe₃	thf	b	6
7	Cs	Ph	SiMe₃	thf	b	6

thf = Tetrahydrofuran, dme = 1,2-dimethoxyethane.

(a)

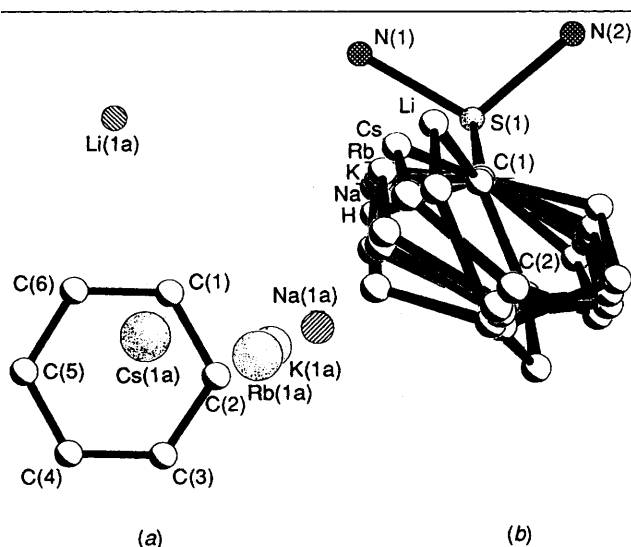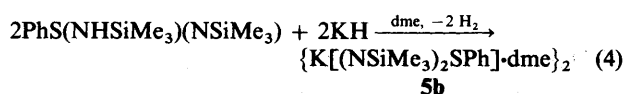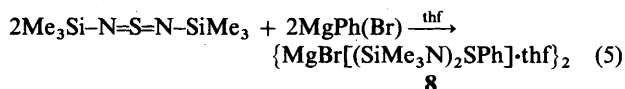**Fig. 2** The bonding of the phenyl ring to the metal atom in compounds **3d, 4a, 5a, 6** and **7** (including the position of the phenyl ring in **1b**)
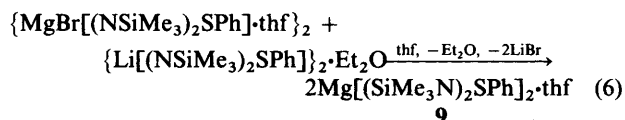
ation of **1a** with KH in hexane–dme leads to the product **5b**, equation (4). The magnesium compound **8** was obtained in a

$$2PhS(NHSiMe_3)(NSiMe_3) + 2KH \xrightarrow{dme, \ -2 H_2}$$
$$\{K[(NSiMe_3)_2SPh] \cdot dme\}_2 \quad (4)$$
$$\mathbf{5b}$$

Grignard reaction with phenylmagnesium bromide and *N,N'*-bis(trimethylsilyl)sulfur diimide in thf according to equation (5).[3] The reaction between **8** and an equimolar amount of **3a**

$$2Me_3Si-N=S=N-SiMe_3 + 2MgPh(Br) \xrightarrow{thf}$$
$$\{MgBr[(SiMe_3N)_2SPh] \cdot thf\}_2 \quad (5)$$
$$\mathbf{8}$$

gave **9** with elimination of LiBr [equation (6)]. Metal exchange

$$\{MgBr[(NSiMe_3)_2SPh] \cdot thf\}_2 +$$
$$\{Li[(NSiMe_3)_2SPh]\}_2 \cdot Et_2O \xrightarrow{thf, \ -Et_2O, \ -2LiBr}$$
$$2Mg[(SiMe_3N)_2SPh]_2 \cdot thf \quad (6)$$
$$\mathbf{9}$$

involving **3a** with Cu^{I}Cl in Et₂O–hexane led to compound **10** [equation (7)], which is slightly sensitive to oxidation and hydrolysis and readily soluble in hydrocarbons.

$$2\{Li[(SiMe_3N)_2SPh]\}_2 \cdot Et_2O + 2CuCl \xrightarrow{-2LiCl}$$
$$\{Cu[(NSiMe_3)_2SPh]\}_2 \quad (7)$$
$$\mathbf{10}$$
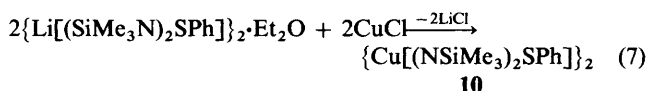
Solid-state Structures.—Crystallographic data for compounds **1a, 2c, 3c, 4b, 5b** and **8–10** are listed in Table 2. For the lithium compounds **2a–2c** and **3a–3e** selected structural parameters are presented in Tables 3 and 4, respectively. Atom coordinates are given in Table 5.

Compound **1a**.The structure of PhS(NHSiMe₃)(NSiMe₃) **1a** (Fig. 3) is very similar to that of PhS(NHBu^t)(NSiMe₃) **1b**.[6] The S–N bonds differ by 9 pm. The N(2) nitrogen atom forms a single bond [166.2(1) pm] to the sulfur atom. The distance between S(1) and N(1) [157.2(1) pm] is not quite consistent with a double bond.[10] In I–N=S=N–I the S–N bonds range from 153(1) to 160(2) pm.[11] Whereas in **1a** the geometry of N(2) is nearly planar, the nitrogen atom in **1b** has a pyramidal environment [deviation of N(2) from the plane of the neighbouring atoms: 7.3 in **1a**, 31.5 pm in **1b**]. Weak hydrogen bridging between H(2n) and N(1a) (214.7 pm) affords dimeriz-
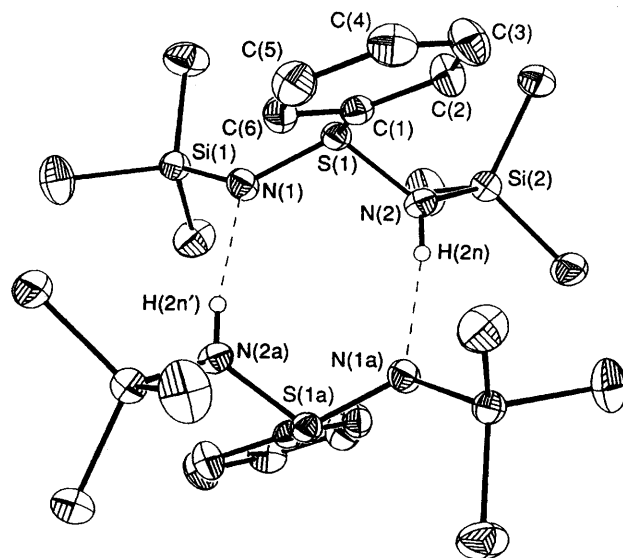

(b)

Fig. 3 The dimeric structure of compound **1a** in the solid. Selected distances (pm) and angles (°): S(1)–N(1) 157.2(1); S(1)–N(2) 166.2(1); S(1)–C(1) 179.9(2); N(1)···H(2n') 214.7; N(1)–S(1)–N(2) 112.1(1); N(1)–S(1)–C(1) 104.3(1); N(2)–S(1)–C(1) 99.6(1)

Table 2 Crystallographic data for compounds 1a, 2c, 3c, 4b, 5b and 8–10 at −120 °C

Compound	1a	2c	3c	4b	5b	8	9	10
Empirical formula	$C_{12}H_{24}N_2SSi_2$	$C_{26}H_{58}Li_2N_4S_2Si_2$	$C_{34}H_{60}Li_2N_4OS_2Si_4$	$C_{28}H_{56}LiN_4NaO_2S_2Si_4$	$C_{32}H_{66}K_2N_4O_4S_2Si_4$	$C_{32}H_{62}Br_2Mg_2N_4OS_2Si_4$	$C_{28}H_{54}Mg_4OS_2Si_4$	$C_{24}H_{46}Cu_2N_4S_2Si_4$
M	284.6	561.0	731.2	687.2	825.6	903.8	680.4	694.2
Crystal dimensions/mm	0.3 × 0.4 × 0.4	0.4 × 0.4 × 0.7	0.3 × 0.4 × 0.5	0.6 × 0.6 × 0.6	0.5 × 0.6 × 0.7	0.6 × 0.6 × 0.7	0.4 × 0.5 × 0.5	0.4 × 0.4 × 0.6
Space group	$P\bar{1}$	$P2_1/n$	$C2/c$	$C222_1$	$P2_1/n$	$P\bar{1}$	$P2_1/n$	$P\bar{1}$
a/pm	952.0(2)	883.4(2)	1943.8(3)	1108.4(2)	1034.8(2)	1083.6(2)	1045.0(2)	981.7(3)
b/pm	975.7(2)	1017.6(2)	1276.2(2)	1920.6(2)	1850.2(3)	1092.5(2)	1845.7(2)	1020.7(3)
c/pm	1053.1(2)	1902.8(2)	1823.3(2)	1924.0(2)	1241.4(3)	1201.0(2)	2006.2(2)	1038.6(3)
α/°	68.83(2)	90	90	90	90	71.85(2)	90	72.07(2)
β/°	75.44(2)	94.49(2)	118.09(2)	90	98.94(2)	88.88(2)	98.11(2)	77.49(2)
γ/°	65.28(2)	90	90	90	90	63.80(2)	90	61.79(2)
U/nm³	0.823	1.705	3.990	4.096	2.348	1.201	3.831	0.869
Z	2	2	4	4	2	1	4	1
D_c/Mg m⁻¹	1.149	1.092	1.150	1.114	1.168	1.272	1.150	1.326
μ/mm⁻¹	0.33	0.25	0.22	0.29	0.42	1.93	0.31	1.50
F(000)	308	616	1464	1480	888	480	1432	364
2θ range/°	8–55	8–55	8–45	8–45	8–45	8–45	8–45	8–45
Number of measured reflections	4234	4370	3565	2972	3339	5101	7093	2422
Number of unique reflections	3772	3899	2589	2663	3041	3120	4977	2251
Number of observed reflections	3529	3432	2306	2618	2866	2900	4482	2209
$F > n\sigma(F)$: n =	4	3	3	3	3	3	3	3
R	0.0280	0.0331	0.0335	0.0228	0.0286	0.0310	0.0443	0.0240
R'	0.0416	0.0429	0.0432	0.0311	0.0396	0.0391	0.0559	0.0418
Goodness of fit S	2.65	1.92	1.71	2.15	2.37	1.99	2.15	2.81
Weighting factor g	0.0001	0.0002	0.0003	0.0001	0.000 15	0.0001	0.0003	0.000 15
Refined parameters	160	166	211	196	221	221	365	165
Data-to-parameter ratio	22.1	20.7	10.9	13.4	13.0	13.1	12.3	13.4
Largest maximum, 10⁻² ρ/e nm⁻³	3.0	3.9	1.9	3.1	2.6	4.4	4.0	3.9
Largest minimum, 10⁻² ρ/e nm⁻³	2.3	3.3	2.7	2.6	2.4	3.4	3.3	2.4
Absorption correction	Semiempirical	—	—	—	—	Semiempirical	—	Semiempirical
η	—	—	—	1.1(2)	—	—	—	—

ation (Fig. 3). The corresponding value in **1b** is slightly longer (219.4 pm).

Compound **2c**. The transannular Li–N distance [216.9(3) pm] in compound **2c** (Fig. 4) is significantly shorter than in the N–SiMe₃ and N–Buᵗ derivatives [237.4(8) and 279.6(9) pm, respectively]. Since all three distances are in the range of normal Li–N contacts in lithium amides,[12] **2c** has to be considered a tricyclic system of three fused four-membered rings (type **b**). The stair angle, *i.e.* that between the Li₂N₂ and SN₂Li planes, assumes a value of 141.6°, which is close to that of the related compound **3d** (144.0°).[9] In **2c** the environment of both lithium atoms in the dimer is equivalent since they are related by a centre of inversion. They exhibit a trigonal non-planar environment. It is expected that **3a**–**3c** give rise to similar structures after removal of ether molecules, as indicated by the solid-state magic angle spinning (MAS) NMR spectra of **3a** and **3c**, which show only one environment for the lithium atoms.

Compound **3c**. Compounds **3a**,[9] **3b**[9] and {Li[PhS(NC₆H₁₁)-(NSiMe₃)]}₂·Et₂O **3c** (Fig. 5) exhibit isotypical **a** type structures: Li(1) is bound to all four nitrogen atoms, Li(2) to the two quaternary nitrogen atoms and the ether molecule. Thus, **3a**–**3c** are rare examples of structures containing lithium atoms in two chemically different environments within the same molecule.[13–17] They are related to the structure of [Li(NBuᵗ)-(OBuᵗ)SiMe₂]₂·thf.[18] In **3c**, Li(1) exhibits a fairly short contact to N(1) [198.8(2) pm], but the Li(1)–N(2) distance [223.3(4)

pm] is rather long due to the additional bonding of N(2) to Li(2) [201.0(3) pm]. The average S–N distance in **3c** is 161.7 pm, 7.1 pm longer than the S=N double bond in S(NSiMe₃)₂.[10] As in **3a**, the alkyl substituent is bonded to the quaternary nitrogen. This feature is all the more remarkable in the NBuᵗ derivative
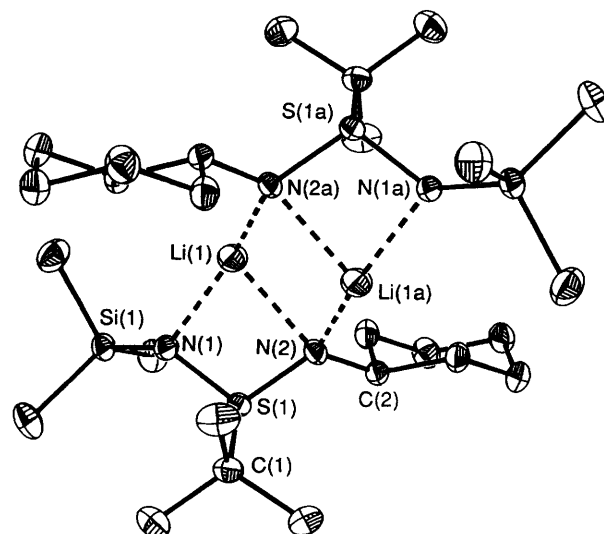

Fig. 4 Crystal structure of compound **2c**

Fig. 5 Crystal structure of compound **3c**

Table 3 Selected bond lengths (pm) and angles (°) for compounds **2a**–**2c**

	2a[a] (R″ = SiMe₃)	**2b**[a] (Buᵗ)	**2c** (C₆H₁₁)
Li(1)–N(1)	191.6(7)	190.4(7)	197.6(3)
Li(1)–N(2a)	196.5(6)	191.2(7)	199.4(3)
Li(1)–N(2)	237.4(8)	(279.6)[b]	216.9(3)
S(1)–N(1)	160.5(3)	160.3(3)	160.8(1)
S(1)–N(2)	162.4(3)	162.5(3)	163.9(1)
S(1)–C(1)	185.4(3)	186.5(3)	185.7(1)
N(1)–Li(1)–N(2a)	140.6(4)	149.1(4)	143.3(1)
N(1)–S(1)–N(2)	105.7(1)	107.1(1)	105.0(1)
N(1)–S(1)–C(1)	104.1(1)	104.1(1)	104.2(1)
N(2)–S(1)–C(1)	103.4(1)	102.0(2)	104.2(1)
C(1)–NSN[c]	113.5	112.4	113.8
NSNLi–NLiNLi[d]	137.5	—	141.6
Ref.	6	6	This work

[a] Average values of three independent molecules; estimated standard deviations (e.s.d.s) reflect the extreme values. [b] Non-bonded distance. [c] Angle between the S(1)–C(1) vector and the plane defined by N(1)–S(1)–N(2). [d] Angle between the four-membered ring units Li(1)–N(1)–S(1)–N(2) and Li(1)–N(2)–Li(1a)–N(2a).
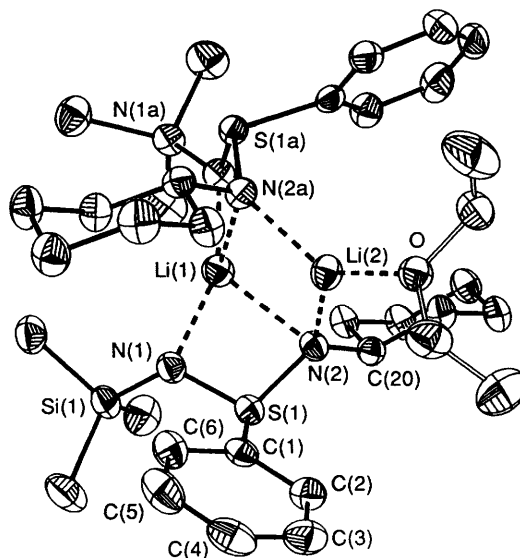
Table 4 Selected bond lengths (pm) and angles (°) for compounds **3a**–**3e** and **4b**

	3a (R″ = SiMe₃)	**3b** (Buᵗ)	**3c** (C₆H₁₁)	**3d** (SiMe₃)	**3e** (SiMe₃)	**4b** (SiMe₃)
Li(1)–N(1)	199.4(3)	198.3(8)	198.8(2)	202.2(5)	212.5(8)[a]	199.4(2)
Li(1)–N(2)	224.5(5)	223.4(13)	223.3(4)	239.3(5)	—	218.8(3)
Li(1)–N(2a)	—	—	—	205.4(5)	—	—
Li(2)[Na(1)[b]]–N(2)	203.3(5)	200.5(11)	201.0(3)	—	—	241.7(2)
Li(1)–O(1)	—	—	—	197.4(5)	—	—
Li(2)[Na(1)[b]]–O(1)	189.7(9)	192.1(19)	194.1(5)	—	235.9(9)[a]	236.9(2)
S(1)–N(1)	159.5(3)	161.3(6)	160.7(2)	159.3(2)	160.1(4)[a]	160.0(2)
S(1)–N(2)	162.3(3)	162.2(6)	162.7(2)	162.7(2)	—	162.2(2)
S(1)–C	180.8(4)	182.6(8)	180.6(2)	180.3(3)	182.0(5)[a]	181.4(2)
N(1)–S(1)–N(2)	105.7(1)	105.6(3)	106.8(1)	105.9(1)	104.4(2)[a]	104.2(1)
N(1)–S(1)–C	104.4(2)	104.1(3)	103.9(1)	104.7(1)	103.4(2)[a]	104.5(1)
N(2)–S(1)–C	101.5(3)	101.5(3)	101.6(1)	104.0(1)	—	102.2(1)
Ref.	9	9	This work	9	7	This work

[a] Average value of chemically equivalent parameters. [b] In **4b**, the sodium atom Na(1) formally replaces Li(2) in **3a**–**3c**.

considering that the bulky *tert*-butyl group is located in the sterically more congested area.

Compound **4b**. Only a few mixed alkali-metal compounds have been reported. We synthesised the derivative LiNa[(Si-Me₃N)₂SPh]·dme **4b** to investigate the influence of a second metal on the bonding properties of the iminoaminosulfinate and obtain a selective and stepwise reactivity of alkali-metal iminoaminosulfinates. Compound **4b** (Fig. 6) exhibits the structural type **a** and, thus, resembles **3a** and **3c**. Formally, Li(2) in **3a** and **3c** has been replaced by a sodium atom, and dme takes the place of the Et₂O molecule. These replacements have little influence on the Li–N distances [Li–N(1) 199.4(2), Li–N(2) 218.8(3) pm; the corresponding values in **3a** are 199.4(3) and 224.5(5) pm, respectively]. The Na–N bond is 241.7(2) pm and, thus, in the normal Na–N range.[19] Both SN₂Li four-membered rings form an angle of 134.3° with the plane of the central N₂LiNa ring. The corresponding angle in **3c** is only 120°. This angle is widened in **4b** because of the larger sodium atom and the increased steric demand of the donor molecule.

Compound **5b**. Despite the increase in the co-ordination number of potassium in {K[(SiMe₃N)₂SPh]·dme}₂ **5b** with respect to {K[(BuᵗN)(SiMe₃N)SPh]·thf}₂ **5a**,[6] due to the use of a bidentate donor molecule there are only minor changes in the overall structure. Unlike **4b**, **5b** (Fig. 7) adopts a type **b** structure in the solid. The K(1)–N(2) contact is longer [305.4(2) pm] than in **5a** [288.0(2) pm], whereas the K(1)–N(1) [272.5(2) pm] and K(1)–N(2a) [282.3(2) pm] distances are even slightly shorter than in the thf adduct [275.2(3) and 288.0(2) pm, respectively].[6] Presumably owing to the higher co-ordination number, the potassium–dme contacts [320.3(2) and 288.5(2) pm] are also longer than the K(1)–O_thf distance [271.6(3) pm] in **5a**. A similar trend can be observed for the potassium–phenyl interaction (376.9 *vs.* 369.8 pm).

Compounds **8** *and* **9**. For {MgBr[(BuᵗN)SBuᵗ]}₂ and similar compounds a dimeric structure with a central eight-membered ring was proposed.[3] The crystal structure of {MgBr[(Si-Me₃N)₂SPh]·thf}₂ **8** reveals a dimer (Fig. 8). The monomeric units are bridged by slightly asymmetric Mg–Br contacts [256.7(1) and 268.1(1) pm], forming a central four-membered Mg₂Br₂ ring. Thus, the structure is different from the ring structure proposed by Kuyper and Vrieze[3] and that of the alkali-metal derivatives, where oligomerization occurs through metal–nitrogen contacts, and represents a new structural type in this class of compounds. The Mg–Br distances are in the range of those for compounds with comparable arrangements.[20,21]

Taking into account the donor thf molecule, the magnesium atoms are five-co-ordinated. The reaction of compound **8** with an equimolar amount of **3a**[9] affords **9**, which is a monomer in
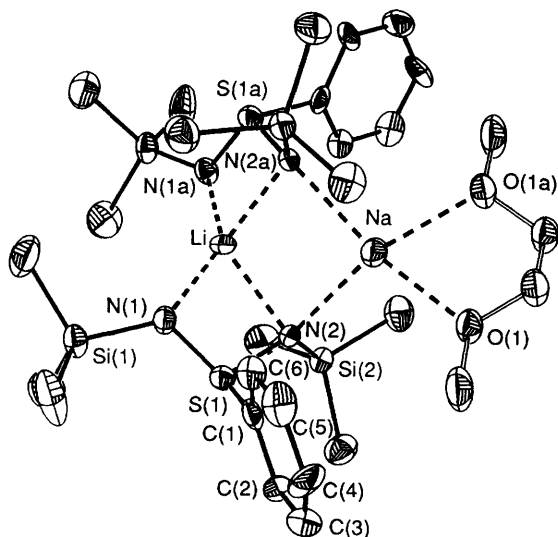
the solid state (Fig. 9). Oligomerization is precluded by the five-co-ordination of the central magnesium atom, which involves all four nitrogen atoms of the two iminoaminosulfinate anions and a thf molecule. A structure of this type, with a donor-free, four-co-ordinate magnesium atom and two chelating monoanionic alkoxysilylamide ligands, was proposed for [Mg{(NBuᵗ)(OBuᵗ)SiMe₂}₂] by Veith and Rösler.[22] These structures are somewhat reminiscent of the situation in the anion in [Li(12-crown-4)₂]⁺[Li{(SiMe₃N)₂SPh}₂]⁻ **3e**.[7]

The Mg–N distances in compound **9** (average 214.2 pm) are *ca.* 5 pm longer than in **8** (average 209.2 pm), presumably due to the electrostatic repulsion between the anions. They are bonded to the same cation in the case of **9**, whereas in **8** they are separated by a Mg₂Br₂ four-membered ring. Likewise, the Mg–O distances differ by a similar amount (*ca.* 6 pm). In both **8** and **9** the two S–N bond lengths in the same anion differ less (1.3 pm in **8**, 0.6 pm in **9**) than in the alkali-metal derivatives,[6,9] presumably owing to the nitrogen atoms having the same co-ordination number.

Whereas the alkali-metal derivatives exhibit N–S–N bond angles between 104.2 and 110.7°,[6] the corresponding values in compounds **8** [98.5(1)°] and **9** [100.1(1)°] are significantly smaller. This can be attributed to the higher charge on Mg²⁺. Thus, the electrostatic repulsion between the metal and the
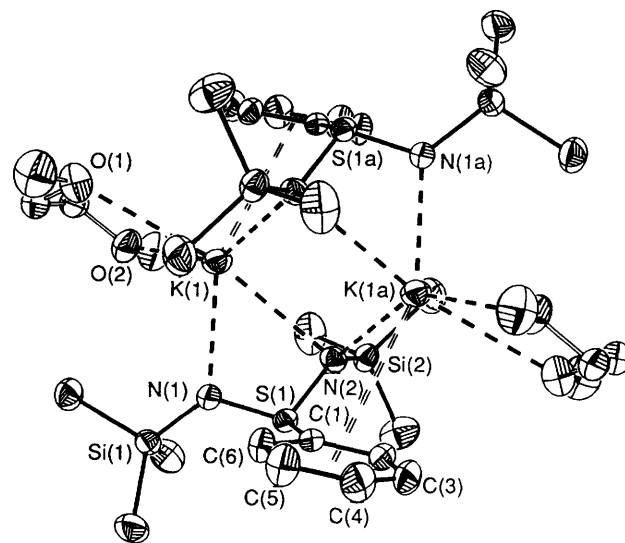
Fig. 7 Crystal structure of compound **5b**. Selected distances (pm) and angles (°): K(1)–N(1) 272.5(2), K(1)–N(2) 305.4(2), K(1)–N(2a) 282.3(2), K(1)–O(1) 320.3(2), K(1)–O(2) 288.5(2), S(1)–N(1) 159.7(2), S(1)–N(2) 161.1(1), S(1)–C(1) 181.2(2), K(1)–Ph_centre 376.9; N(1)–S(1)–N(2) 110.2(1), N(1)–S(1)–C(1) 102.8(1), N(2)–S(1)–C(1) 100.6(1)

Fig. 6 Crystal structure of compound **4b**
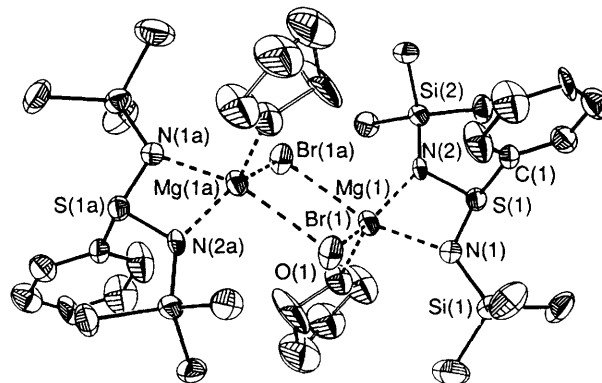
Fig. 8 Crystal structure of compound **8**. Selected distances (pm) and angles (°): Mg(1)–N(1) 210.6(3), Mg(1)–N(2) 207.8(2), Mg(1)–Br(1) 256.7(1), Mg(1)–Br(1a) 268.1(1), Mg(1)–O(1) 201.4(2), S(1)–N(1) 160.3(2), S(1)–N(2) 161.6(3); N(1)–Mg(1)–N(2) 71.3(1), N(1)–S(1)–N(2) 98.5(1)

Fig. 9 Crystal structure of compound **9**. Selected distances (pm) and angles (°): Mg–N(1) 218.9(2), Mg–N(2) 209.8(2), Mg–N(3) 217.5(2), Mg–N(4) 210.7(2), Mg–O 207.4(2), S(1)–N(1) 161.1(2), S(1)–N(2) 161.7(2), S(2)–N(3) 161.4(2), S(2)–N(4) 161.9(2); N(1)–Mg–N(2) 70.5(1), N(3)–Mg–N(4) 70.7(1), N(1)–S(1)–N(2) 100.1(1), N(3)–S(2)–N(4) 100.0(1)
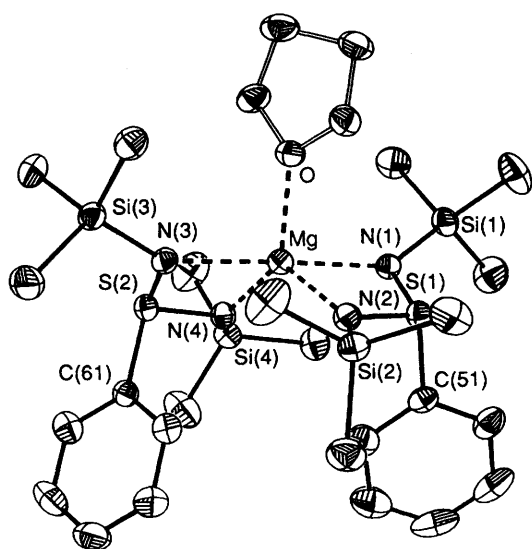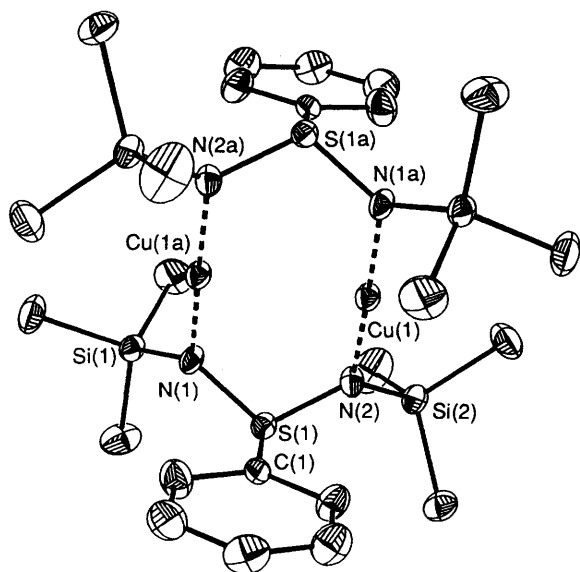

Fig. 10 Crystal structure of compound **10**. Selected distances (pm) and angles (°): Cu(1)–N(1) 187.3(2), Cu(1)–N(2a) 187.4(2); Cu(1) · · · Cu(1a) 270.2(1), S(1)–N(1) 161.3(2), S(1)–N(2) 162.5(3), N(1)–Cu(1)–N(2a) 178.6(1), N(1)–S(1)–N(2) 110.4(1)

sulfur atom is higher in the cases of **8** and **9**. This observation is in accord with the N–Si–N angle in {Mg[(Bu^{t}N)$_2$SiMe$_2$]·thf}$_2$,[23] which is also considerably smaller (99.9°) than in a monoanionic alkoxysilylamide system with alkali metals as counter cations (average 106.5°).[18,24]

The reaction of Grignard reagents with the sulfur diimide system leads to structures different from those of the corresponding alkali-metal derivatives. Further investigations of metal-exchange reactions and other alkaline-earth metal iminoaminosulfinates are underway.

Compound **10**. The structure of compound **10** in the solid state shows a dimeric, c-type arrangement (Fig. 10). No transannular Cu–N contacts are present. The Cu atoms show a linear environment [N–Cu–N 178.6(1)°] of the symmetrically bonded N atoms [Cu(1)–N(1) 187.3(2), Cu(1)–N(2a) 187.4(2) pm]. The transannular Cu · · · Cu distance [270.2(1) pm] is longer than in
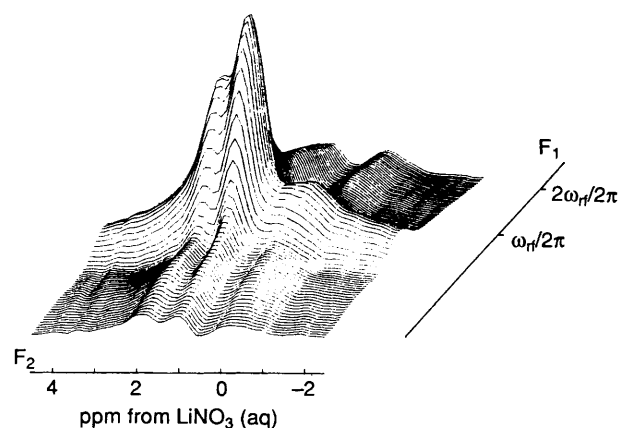
the isotypical copper benzamidinate[25] [242.5(2) pm], due to the greater cone angle of the N–S–N system, and is too long to be considered as a metal–metal interaction, as there is in the three-centre two-electron bond in [Li(thf)$_4$][Cu$_5$Cl$_4$-{Si(SiMe$_3$)$_3$}$_2$] with a Cu–Cu bond of 240.3(2) pm.[26]

Solid-state MAS NMR Investigations of Compounds **3a** *and* **3c**.—Solution NMR data for {Li[(SiMe$_3$N)$_2$SPh]}$_2$·Et$_2$O **3a** have been published.[9] This compound exhibits two signals in the ^{7}Li NMR spectrum in C$_7$D$_8$ at -60 °C (δ 1.2, 2.7 in a 1:1 ratio). At this temperature two signals for the chemically non-equivalent silyl groups can be resolved in the ^{1}H NMR spectrum. Conversely, the ^{6}Li,^{1}H Heteroatom Overhauser Effect Spectroscopy (HOESY) NMR spectrum of {Li[(Bu^{t}N)-(SiMe$_3$N)SPh]}$_2$·Et$_2$O **3b**[9] exhibits exchange of the Bu^t and the Me$_3$Si groups even at -70 °C. Within the NMR time-scale, the chemical shifts for both groups show identical cross-peaks with both ^{6}Li signals.

For [Li(12-crown-4)$_2$]$^+$[Li{(SiMe$_3$N)$_2$SPh}$_2$]$^-$ **3e** it was possible for the first time to resolve and assign three different lithium-7 environments in a ^{7}Li MAS NMR experiment.[7] Solid-state NMR spectroscopy is a versatile physical method by which phase transformations may be investigated. Lithium-7 quadrupole nutation MAS NMR spectroscopy was also applied to **3c** (Fig. 11). The two-dimensional spectrum was recorded with a 91 ± 5 kHz radiofrequency excitation field, $\omega_{rf}/2\pi$, 5 s recycle delay and ca. 3.5 kHz spinning rate. The F$_2$ axis of two-dimensional NMR spectra consists of a combination of chemical shift and second-order quadrupolar shift, whereas the F$_1$ axis includes only quadrupolar information. This method allows lithium-7 environments with different quadrupolar coupling constants C_Q along F$_1$ to be resolved.[27] Unexpectedly, the spectrum shows three signals instead of two. Owing to their width and partial overlap we refrain from quoting chemical shifts. However, the spectrum clearly shows three ^{7}Li nuclei in different environments.

Removing the clear, colourless crystals of compounds **3a** and **3c** from the mother-liquor causes withering and transformation into a yellow amorphous powder, which is insoluble in non-polar solvents. This transformation had progressed significantly at the time of the experiment depicted in Fig. 11. The two signals of the starting material and that of the transformation product are discernible.

We repeated the solid-state MAS NMR experiment and produced one-dimensional ^{7}Li MAS spectra in order to account for the transformation in detail (Fig. 12). As expected two signals can be seen. A third peak begins to appear after evacuating both samples for 24 h. For compound **3a**, after heating to ca. 50 °C and 10^{-2} bar for 10 min, both original signals have disappeared and a new one (b) has formed. When the same experiment was performed on **3c** the original signals

Fig. 11 Lithium-7 quadrupole nutation MAS NMR spectrum of compound **3c**

were still present, but the peak assigned to the transformation product is predominant (d). This experiment clearly indicates that the two different lithium-7 environments in **3a** and **3c** are no longer present in the product. Therefore, there can be only one type of environment for the lithium atom in the product. In our opinion, the ether molecule is released into the gas phase and the dimers have to reorganize (Scheme 1). The bond between one nitrogen atom and the four-co-ordinate lithium atom opens. One anionic monomer rotates around the remaining Li–N bonds, and the nitrogen atom attached to the lithium atom from which the ether molecule has been removed. The plausibility of this transformation is supported by the knowledge of the structural type of the product.

Conclusion

The iminoaminosulfinate anion has proven to be versatile for the steric stabilization of metal derivatives, even in less-stable oxidation states, as exemplified by the copper derivative **10**. It enables a favourable solubility in non-polar solvents. In contrast to an analogous series of alkali-metal iminoaminophosphinates,[28] the class of compounds presented here is structurally homogeneous within the first main-group derivatives. Varying the substituent at one or both nitrogen atoms as well as at the sulfur atom allows excellent fine-tuning of the steric requirement of the sulfinate. Furthermore, it exhibits a variety of structural features and, by virtue of the properties of its substituents, is readily accessible to NMR studies at different temperatures and transition phases. Further investigations of metal-exchange reactions and of pathways leading to anions with 'inorganic' substituents at S are underway.

Experimental

All experiments were carried out under dry argon with strict exclusion of air and moisture. Mass spectra: Varian CH5 spectrometer. NMR: ^{1}H, ^{7}Li, ^{13}C, 10% solutions in $C_6D_5CD_3$ (^{1}H of **9** in C_6D_6, **8** in C_4D_8O); ^{29}Si, 20% solutions in $C_6D_5CD_3$, SiMe$_4$, LiCl external, Bruker AM 250 spectrometer.

The compound PhS(NHSiMe$_3$)(NSiMe$_3$) **1a** was prepared according to literature procedures.[6]

*Syntheses.—Compound **2c**.* The compound C_6H_{11}–N=S=O was prepared according to literature procedures;[29] C_6H_{11}–N=S=N–SiMe$_3$ was prepared analogously to the corresponding Bu^t and Et derivatives.[30,31] The compound C_6H_{11}–N=S=N–SiMe$_3$ (0.01 mol) was dissolved in pentane (50 cm^3) and cooled to -60 °C. *tert*-Butyllithium (0.01 mol, 1.5 mol dm^{-3} solution in pentane) and Et$_2$O (0.04 mol) were added dropwise. The reaction mixture was allowed to warm to room temperature and refluxed for 1 h. After 4 d single crystals of compound **2c** suitable for X-ray analysis were obtained. Yield: 2.4 g, 86% (room temperature): ^{1}H, δ 0.27 (s, SiMe$_3$), 0.88–1.73 (m, C$_6$H$_{11}$), 1.05 and 1.07 (s, SBu^t); ^{7}Li, δ 1.7; ^{13}C, δ 3.25, 3.36 [Si(CH$_3$)$_3$], 22.93, 23.29 [SC(CH$_3$)$_3$], 28.14 [SC(CH$_3$)$_3$], 37.24, 37.55, 39.45, 55.25, 55.70, 61.05 and 61.20 (C$_6$H$_{11}$); ^{29}Si, δ -4.4.

*Compound **3c**.* The compound C_6H_{11}–N=S=N–SiMe$_3$ (0.02 mol) was dissolved in hexane (50 cm^3) and cooled to -50 °C. A 2 mol dm^{-3} solution of LiPh (10 cm^3) in hexane–Et$_2$O was added dropwise. After warming to room temperature, the reaction mixture was refluxed for 1 h. After 2 d single crystals of compound **3c** suitable for X-ray analysis were obtained. Yield: 6.3 g, 93%. NMR (room temperature): ^{1}H, δ 0.26 (s, SiMe$_3$), 0.80–1.85 (m, C$_6$H$_{11}$) and 6.97–7.80 (m, C$_6$H$_5$); ^{7}Li, δ 1.5; ^{13}C, δ 2.84 [Si(CH$_3$)$_3$], 15.20 [O(CH$_2$CH$_3$)$_2$], 37.57, 38.85, 40.89, 61.43 (C$_6$H$_{11}$), 65.35 [O(CH$_2$CH$_3$)$_2$], 126.23, 128.41, 129.18 and 146.10 (C$_6$H$_5$); ^{29}Si, δ -4.2.

*Compound **4b**.* The compound PhS(NHSiMe$_3$)(NSiMe$_3$) (0.01 mol) was dissolved in hexane (20 cm^3) and added dropwise to a suspension of NaH (0.011 mol) and {Li[(SiMe$_3$N)$_2$SPh]}$_2$· Et$_2$O (0.005 mol) in hexane (20 cm^3) and dme (0.04 mol). After
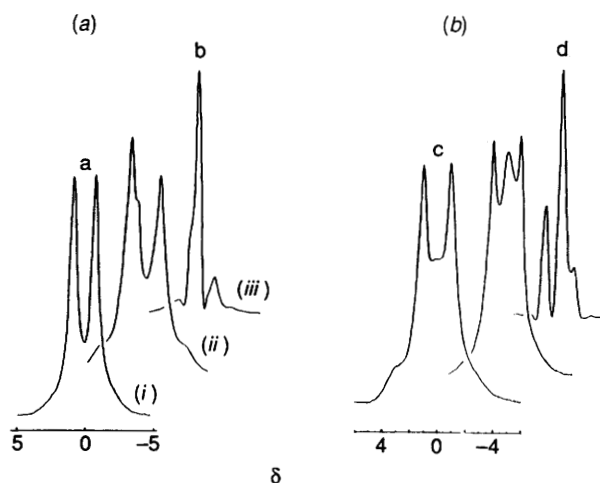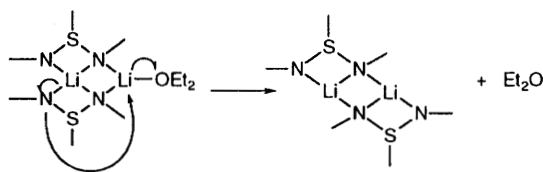

Fig. 12 Solid-state ^{7}Li MAS NMR spectra of compounds **3a** (*a*) and **3c** (*b*): (*i*) sample from mother-liquor; (*ii*) after 24 h at 10^{-2} bar; (*iii*) after heating at 10^{-2} bar

Scheme 1 Reorganization of an **a** to a **b**-type structure after release of the donor molecule

cooling the excess of NaH was filtered off. The solution was kept at -35 °C for 10 d until crystals suitable for X-ray crystallography were obtained. NMR (room temperature): ^{1}H, δ 0.29 (s, SiMe$_3$), 2.94 [s, CH$_3$O(CH$_2$)$_2$OCH$_3$], 2.99 [s, CH$_3$O(CH$_2$)$_2$OCH$_3$] and 6.99–7.82 (m, C$_6$H$_5$); ^{7}Li, δ 1.8; ^{13}C, δ 3.21 [Si(CH$_3$)$_3$], 58.60, 71.17 (dme), 125.69, 127.88, 128.42 and 159.12 (C$_6$H$_5$); ^{29}Si, δ -4.2.

*Compound **5b**.* The compound PhS(NHSiMe$_3$)(NSiMe$_3$) (0.01 mol) was dissolved in hexane (20 cm^3) and added dropwise to a suspension of KH (0.011 mol) in hexane (10 cm^3) and dme (0.04 mol). The reaction mixture was refluxed for 2 h. After cooling, the excess of KH was filtered off. The solution was kept at -35 °C for several weeks to grow crystals of compound **5b** suitable for X-ray crystallography. Yield: 3.4 g, 83%. NMR (room temperature): ^{1}H, δ 0.26 (s, SiMe$_3$), 3.10 [s, CH$_3$O(CH$_2$)$_2$OCH$_3$] and 3.26 [s, CH$_3$O(CH$_2$)$_2$OCH$_3$].

*Compound **8**.* Bromobenzene (0.01 mol) was added dropwise to magnesium turnings (0.01 mol) in Et$_2$O (20 cm^3). The reaction mixture was refluxed for 1 h, transferred to a dropping funnel, and added to Me$_3$Si–N=S=N–SiMe$_3$ (0.01 mol) in hexane (50 cm^3). Compound **8** was precipitated from the solution and can be dissolved by addition of thf (1.5 g). Single crystals suitable for X-ray crystallography were obtained from this solution at -20 °C. Yield: 3.0 g, 90%. NMR (C$_4$D$_8$O, room temperature): ^{1}H, δ 0.00 (s, SiMe$_3$), 1.73 [t, O(CH$_2$)$_2$(CH$_2$)$_2$], 3.58 [t, O(CH$_2$)$_2$(CH$_2$)$_2$] and 7.10–7.95 (m, C$_6$H$_5$); ^{13}C, δ 1.98 (SiMe$_3$), 25.26 [O(CH$_2$)$_2$(CH$_2$)$_2$], 67.52 [O(CH$_2$)$_2$(CH$_2$)$_2$], 128.25, 129.92 and 132.49 (C$_6$H$_5$).

*Compound **9**.* A solution of compound **8** (0.01 mol) was added dropwise to an equimolar solution of **3a**. This mixture was stirred for 12 h, after which the solvents were removed *in vacuo*. Redissolving the product in hexane (50 cm^3) and filtering off the LiBr afforded crystals of **9** suitable for X-ray structure determination. Yield: 3.6 g, 54%. NMR (room temperature): ^{1}H, δ 0.20 (s, SiMe$_3$), 1.42 [t, O(CH$_2$)$_2$(CH$_2$)$_2$], 3.63 [t, O(CH$_2$)$_2$(CH$_2$)$_2$] and 6.99–7.94 (m, C$_6$H$_5$); ^{13}C, δ 2.39 (SiMe$_3$), 25.58 [O(CH$_2$)$_2$(CH$_2$)$_2$], 68.28 [O(CH$_2$)$_2$(CH$_2$)$_2$], 124.31, 129.08, 130.34 and 155.91 (C$_6$H$_5$); ^{29}Si, δ -2.6 (SiMe$_3$).

*Compound **10**.* The compound Me$_3$Si–N=S=N–SiMe$_3$ (0.005

Table 5 Atom coordinates ($\times 10^4$)

Atom	x	y	z	Atom	x	y	z
Compound 1a							
S(1)	5 211(1)	2 526(1)	6 293(1)	C(7)	3 390(2)	5 029(2)	8 897(2)
C(1)	5 098(2)	2 271(1)	4 718(1)	C(8)	633(2)	5 222(2)	7 852(2)
C(2)	6 377(2)	1 212(2)	4 159(2)	C(9)	2 897(2)	2 034(2)	9 251(2)
C(3)	6 260(2)	911(2)	3 005(2)	N(2)	6 813(1)	2 958(1)	5 845(1)
C(4)	4 880(2)	1 653(2)	2 424(2)	Si(2)	8 339(1)	1 975(1)	6 858(1)
C(5)	3 610(2)	2 699(2)	2 991(2)	C(10)	7 742(2)	2 288(2)	8 580(2)
C(6)	3 710(2)	3 003(2)	4 153(1)	C(11)	9 043(2)	−184(2)	7 081(2)
N(1)	3 708(1)	3 992(1)	6 465(1)	C(12)	9 893(2)	2 770(2)	5 897(2)
Si(1)	2 727(1)	4 044(1)	8 075(1)				
Compound 2c							
S(1)	5 602(1)	4 194(1)	3 671(1)	C(13)	5 946(2)	6 761(2)	2 186(1)
C(1)	3 674(2)	3 617(1)	3 355(1)	N(2)	5 754(1)	3 820(1)	4 512(1)
C(14)	3 681(2)	2 133(1)	3 466(1)	C(2)	6 916(2)	2 771(1)	4 651(1)
C(15)	2 472(2)	4 283(2)	3 761(1)	C(21)	6 515(2)	1 946(1)	5 283(1)
C(16)	3 465(2)	3 961(2)	2 573(1)	C(22)	7 690(2)	861(1)	5 451(1)
N(1)	5 474(1)	5 771(1)	3 649(1)	C(23)	9 283(2)	1 426(2)	5 573(1)
Si(1)	6 629(1)	6 664(1)	3 141(1)	C(24)	9 703(2)	2 242(2)	4 943(1)
C(11)	8 610(2)	5 995(2)	3 187(1)	C(25)	8 528(2)	3 322(1)	4 772(1)
C(12)	6 661(2)	8 375(2)	3 502(1)	Li(1)	5 537(3)	5 915(2)	4 686(1)
Compound 3c							
S(1)	4 766(1)	5 594(1)	5 997(1)	N(2)	5 326(1)	4 893(1)	6 806(1)
C(1)	3 947(1)	4 725(2)	5 451(1)	C(20)	6 144(1)	4 856(2)	6 944(1)
C(2)	4 076(1)	3 810(2)	5 124(1)	C(21)	6 549(1)	3 914(2)	7 482(1)
C(3)	3 456(1)	3 153(2)	4 654(1)	C(22)	7 399(1)	3 834(2)	7 674(1)
C(4)	2 718(1)	3 404(2)	4 520(1)	C(23)	7 844(1)	4 823(2)	8 085(2)
C(5)	2 592(1)	4 301(2)	4 856(1)	C(24)	7 458(1)	5 779(2)	7 550(2)
C(6)	3 209(1)	4 980(2)	5 320(1)	C(25)	6 602(1)	5 857(2)	7 350(1)
N(1)	4 418(1)	6 520(1)	6 321(1)	Li(1)	5 000	6 064(4)	7 500
Si(1)	4 211(1)	7 729(1)	5 865(1)	Li(2)	5 000	4 004(4)	7 500
C(11)	3 872(1)	8 530(2)	6 490(2)	O	5 000	2 483(2)	7 500
C(12)	3 441(2)	7 694(2)	4 752(2)	C(7)	4 522(1)	1 878(2)	6 772(1)
C(13)	5 080(2)	8 367(2)	5 868(2)	C(8)	4 967(2)	1 341(3)	6 408(2)
Compound 4b							
Na	5 000	6 381(1)	2 500	C(11)	5 704(3)	8 994(1)	4 773(1)
Li	5 000	7 930(2)	2 500	C(12)	6 245(3)	9 600(1)	3 343(2)
S(1)	3 896(1)	7 794(1)	3 707(1)	C(13)	3 694(2)	9 621(1)	3 918(1)
C(1)	4 598(2)	7 265(1)	4 375(1)	N(2)	3 766(1)	7 248(1)	3 069(1)
C(2)	3 868(2)	6 982(1)	4 887(1)	Si(2)	2 313(1)	7 113(1)	2 766(1)
C(3)	4 369(2)	6 581(1)	5 407(1)	C(21)	1 223(2)	6 856(1)	3 462(1)
C(4)	5 595(2)	6 448(1)	5 406(1)	C(22)	2 407(2)	6 373(1)	2 135(1)
C(5)	6 326(2)	6 734(1)	4 896(1)	C(23)	1 734(2)	7 908(1)	2 311(1)
C(6)	5 823(2)	7 150(1)	4 384(1)	O(1)	4 568(2)	5 369(1)	3 158(1)
N(1)	4 937(2)	8 316(1)	3 462(1)	C(7)	4 554(3)	5 374(1)	3 898(1)
Si(1)	5 121(1)	9 107(1)	3 862(1)	C(8)	5 088(2)	4 748(1)	2 887(1)
Compound 5b							
K(1)	−447(1)	11 059(1)	−625(1)	C(13)	−5 029(2)	10 235(1)	−3 288(2)
S(1)	−1 821(1)	9 543(1)	−2 027(1)	N(2)	−303(1)	9 519(1)	−1 485(1)
C(1)	−2 548(2)	9 014(1)	−1 049(1)	Si(2)	840(1)	9 404(1)	−2 331(1)
C(2)	−2 129(2)	8 303(1)	−841(2)	C(21)	2 411(2)	9 168(1)	−1 446(2)
C(3)	−2 711(2)	7 883(1)	−127(2)	C(22)	409(2)	8 680(1)	−3 375(2)
C(4)	−3 707(2)	8 162(1)	375(2)	C(23)	1 171(2)	10 239(1)	−3 087(2)
C(5)	−4 133(2)	8 860(1)	155(2)	C(7)	−2 016(3)	12 801(2)	764(2)
C(6)	−3 559(2)	9 283(1)	−563(2)	O(1)	−1 116(2)	12 673(1)	37(1)
N(1)	−2 408(1)	10 331(1)	−1 897(1)	C(8)	−1 395(2)	13 118(1)	−897(2)
Si(1)	−3 408(1)	10 701(1)	−2 978(1)	C(9)	−357(2)	13 042(1)	−1 580(2)
C(11)	−2 672(2)	10 702(1)	−4 259(2)	O(2)	−307(1)	12 324(1)	−1 961(1)
C(12)	−3 695(2)	11 656(1)	−2 592(2)	C(10)	549(3)	12 268(1)	−2 748(2)
Compound 8							
S(1)	2 292(1)	4 324(1)	8 335(1)	N(2)	1 660(2)	3 393(2)	7 963(2)
C(1)	3 988(3)	3 767(3)	7 839(2)	Si(2)	2 161(1)	1 600(1)	8 747(1)
C(2)	4 149(3)	3 793(5)	6 704(3)	C(21)	585(3)	1 322(4)	8 915(3)
C(3)	5 452(4)	3 346(5)	6 366(3)	C(22)	3 330(3)	448(4)	7 934(3)
C(4)	6 586(3)	2 908(4)	7 139(3)	C(23)	3 074(3)	1 077(4)	10 244(3)
C(5)	6 426(3)	2 894(4)	8 270(3)	Mg(1)	302(1)	5 100(1)	6 517(1)
C(6)	5 125(3)	3 327(3)	8 626(3)	Br(1)	267(1)	6 586(1)	4 377(1)
N(1)	1 316(2)	5 881(3)	7 381(2)	O(1)	−1 655(2)	6 120(3)	6 849(2)
Si(1)	1 397(1)	7 439(1)	7 320(1)	C(7)	−2 892(4)	7 067(6)	6 003(4)
C(11)	2 475(4)	7 856(4)	6 181(3)	C(8)	−3 918(4)	7 826(7)	6 680(6)
C(12)	2 193(4)	7 228(4)	8 770(3)	C(9)	−3 552(4)	6 656(6)	7 920(5)
C(13)	−375(4)	8 956(4)	6 901(4)	C(10)	−2 034(4)	5 876(6)	8 029(4)

Table 5 (*continued*)

Atom	x	y	z	Atom	x	y	z
Compound 9				C(63)	5 519(3)	5 425(2)	6 915(2)
S(1)	4 348(1)	8 390(1)	5 784(1)	C(64)	5 475(3)	4 681(2)	6 860(2)
C(51)	5 483(3)	7 885(2)	5 362(1)	C(65)	4 346(3)	4 334(2)	6 609(2)
C(52)	5 594(3)	7 140(2)	5 406(2)	C(66)	3 242(3)	4 737(2)	6 402(1)
C(53)	6 451(3)	6 788(2)	5 049(2)	N(3)	1 752(2)	6 620(1)	6 688(1)
C(54)	7 178(3)	7 173(2)	4 656(2)	Si(3)	942(1)	6 419(1)	7 359(1)
C(55)	7 088(3)	7 915(2)	4 620(2)	C(31)	664(3)	7 281(2)	7 802(1)
C(56)	6 239(3)	8 274(2)	4 975(2)	C(32)	−653(3)	5 978(2)	7 070(2)
N(1)	2 971(2)	8 247(1)	5 332(1)	C(33)	1 907(3)	5 794(2)	7 974(2)
Si(1)	2 362(1)	8 873(1)	4 728(1)	N(4)	2 272(2)	6 475(1)	5 528(1)
C(11)	3 185(3)	8 866(2)	3 961(2)	Si(4)	2 035(1)	6 126(1)	4 720(1)
C(12)	621(3)	8 652(2)	4 473(2)	C(41)	2 706(3)	6 780(2)	4 158(2)
C(13)	2 514(4)	9 825(2)	5 064(2)	C(42)	276(3)	5 986(2)	4 423(2)
N(2)	4 171(2)	7 916(1)	6 443(1)	C(43)	2 836(4)	5 231(2)	4 671(2)
Si(2)	5 188(1)	8 047(1)	7 192(1)	Mg	2 377(1)	7 467(1)	6 052(1)
C(21)	6 696(3)	7 499(2)	7 222(2)	O	962(2)	8 170(1)	6 293(1)
C(22)	5 645(3)	9 018(2)	7 314(2)	C(71)	1 249(3)	8 887(2)	6 577(2)
C(23)	4 281(3)	7 744(2)	7 873(2)	C(72)	23(3)	9 311(2)	6 398(2)
S(2)	1 844(1)	5 994(1)	6 134(1)	C(73)	−1 005(3)	8 735(2)	6 437(2)
C(61)	3 287(3)	5 486(2)	6 446(1)	C(74)	−427(3)	8 072(2)	6 151(2)
C(62)	4 423(3)	5 830(2)	6 710(2)				
Compound 10							
Cu(1)	6 554(1)	4 445(1)	4 717(1)	Si(1)	7 301(1)	6 086(1)	1 782(1)
S(1)	4 658(1)	7 743(1)	3 521(1)	C(11)	7 105(3)	8 001(3)	729(3)
C(1)	4 866(3)	7 964(3)	5 115(2)	C(12)	9 360(3)	4 817(3)	2 157(3)
C(2)	3 557(3)	8 599(3)	5 963(3)	C(13)	6 705(3)	5 162(3)	854(3)
C(3)	3 717(3)	8 802(3)	7 167(3)	N(2)	3 184(2)	7 337(2)	3 917(2)
C(4)	5 156(3)	8 384(3)	7 527(3)	Si(2)	1 650(1)	8 328(1)	2 897(1)
C(5)	6 457(3)	7 768(3)	6 670(3)	C(21)	756(3)	10 416(3)	2 817(3)
C(6)	6 314(3)	7 561(3)	5 466(3)	C(22)	2 234(4)	8 093(4)	1 123(3)
N(1)	6 242(2)	6 236(2)	3 351(2)	C(23)	228(3)	7 533(3)	3 719(3)

mol) was dissolved in hexane (20 cm^3) and cooled to $-30\,^\circ$C. To this solution anhydrous CuCl (0.005 mol) was added followed by 0.005 mol LiPh (2 mol dm^{-3} solution in hexane–Et$_2$O) dropwise. After warming to room temperature, the reaction mixture was refluxed for 2 h. After cooling the LiCl was filtered off. Crystals of compound **10** were obtained by allowing the solution to stand for 12 h. Yield: 1.3 g, 74%. M.p. 141 $^\circ$C (decomp.). NMR (room temperature): ^{1}H, δ 0.21 (s, SiMe$_3$) and 7.00–7.95 (m, C$_6$H$_5$); ^{13}C, δ 2.72 [Si(CH$_3$)$_3$], 126.20, 128.41, 128.57 and 156.10 (C$_6$H$_5$); ^{29}Si, δ 5.1 (SiMe$_3$). Mass spectra: (electron impact) m/z 694 (18), 617 (100); (field ionization) 694 (100%). IR: 2949vs, 1472m, 1442m, 1260s, 1249vs, 1095m, 988vs, 964vs, 866vs, 833vs, 745vs, 684s, 452m and 321m cm^{-1}.

Crystal Structure Determinations of Compounds **1a, 2c, 3c, 4b, 5b** *and* **8–10**.—Data were collected on a Stoe-Siemens AED diffractometer using graphite-monochromated Mo-Kα radiation ($\lambda = 71.073$ pm). The structures of compounds **8** and **10** were solved by the Patterson method, those of **1a, 2c, 3c, 4b, 5b** and **9** by direct methods.[32] They were refined by full-matrix least-squares techniques.[33] All non-hydrogen atoms were refined anisotropically. Hydrogen atoms were included in calculated positions. A semiempirical absorption correction was applied for **8** and **10**. A weighting scheme $w^{-1} = \sigma^2(F) + gF^2$ was employed.

Additional material available from the Cambridge Crystallographic Data Centre comprises H-atom coordinates, thermal parameters and remaining bond lengths and angles.

Acknowledgements

References

1 U. Wannagat and H. Kuckertz, *Angew. Chem.*, 1962, **74**, 117.
2 O. J. Scherer and R. Schmitt, *J. Organomet. Chem.*, 1969, **16**, P11.
3 J. Kuyper and K. Vrieze, *J. Chem. Soc., Chem. Commun.*, 1976, 64.
4 J. Kuyper, P. C. Keijzer and K. Vrieze, *J. Organomet. Chem.*, 1976, **116**, 1.
5 O. Scherer and R. Wies, *Z. Naturforsch., Teil B*, 1970, **25**, 1486.
6 F. Pauer and D. Stalke, *J. Organomet. Chem.*, 1991, **418**, 127.
7 F. Pauer, J. Rocha and D. Stalke, *J. Chem. Soc., Chem. Commun.*, 1991, 1477.
8 E. Eaborn, P. B. Hitchcock, J. D. Smith and A. C. Sullivan, *J. Chem. Soc., Chem. Commun.*, 1983, 827.
9 F. T. Edelmann, F. Knösel, F. Pauer, D. Stalke and W. Bauer, *J. Organomet. Chem.*, 1992, **438**, 1.
10 D. G. Anderson, H. E. Robertson, D. W. H. Rankin and J. D. Woollins, *J. Chem. Soc., Dalton Trans.*, 1989, 859.
11 M. Rock, P. Bravin and K. Seppelt, *Z. Anorg. Allg. Chem.*, 1992, **618**, 89.
12 K. Gregory, P. v. R. Schleyer and R. Snaith, *Adv. Inorg. Chem.*, 1991, **37**, 47.
13 E. Weiss, G. Sauermann and G. Thirase, *Chem. Ber.*, 1983, **116**, 74.
14 W. Clegg, R. E. Mulvey, R. Snaith, G. E. Toogood and K. Wade, *J. Chem. Soc., Chem. Commun.*, 1986, 1740.
15 U. Schümann and E. Weiss, *Angew. Chem.*, 1988, **100**, 573; *Angew. Chem., Int. Ed. Engl.*, 1988, **27**, 584.
16 D. Barr, W. Clegg, R. E. Mulvey and R. Snaith, *J. Chem. Soc., Chem. Commun.*, 1989, 57.
17 G. Boche, H. Etzrod, W. Massa and G. Baum, *Angew. Chem.*, 1985, **97**, 858; *Angew. Chem., Int. Ed. Engl.*, 1985, **24**, 863.
18 M. Veith and J. Böhnlein, *Chem. Ber.*, 1989, **122**, 603.
19 D. Stalke, M. Wedler and F. T. Edelmann, *J. Organomet. Chem.*, 1992, **431**, C1.
20 A. L. Spek, P. Voorbergen, G. Schat, C. Blomberg and F. Bickelhaupt, *J. Organomet. Chem.*, 1974, **77**, 147.
21 K. Prout and R. A. Forder, *Acta Crystallogr., Sect. B*, 1967, **31**, 852.
22 M. Veith and R. Rösler, *J. Organomet. Chem.*, 1982, **229**, 131.

23 M. Veith, W. Frank, F. Töllner and H. Lange, *J. Organomet. Chem.*, 1987, **326**, 315.

24 M. Veith, J. Böhnlein and V. Huch, *Chem. Ber.*, 1989, **122**, 841.

25 S. Maier, W. Hiller, J. Strähle, C. Ergezinger and K. Dehnicke, *Z. Naturforsch., Teil B*, 1988, **43**, 1628.

26 A. Heine and D. Stalke, *Angew. Chem.*, 1993, **105**, 90; *Angew. Chem., Int. Ed. Engl.*, 1993, **32**, 121.

27 A. Samoson and E. Lippmaa, *J. Magn. Reson.*, 1988, **78**, 255.

28 A. Steiner and D. Stalke, *Inorg. Chem.*, 1993, **32**, 1977.

29 D. Klamann, C. Sass and M. Zelenka, *Chem. Ber.*, 1959, **92**, 1910.

30 I. Ruppert, V. Bastian and R. Appel, *Chem. Ber.*, 1975, **108**, 2329.

31 F. Pauer, Dissertation, University of Göttingen, 1991.

32 G. M. Sheldrick, *Acta Crystallogr., Sect. A*, 1990, **46**, 467.

33 SHELXTL PLUS, G. M. Sheldrick, University of Göttingen, 1986.